



# OPEN Effects of long-term neural adaptation to habitual spherical aberration on through-focus visual acuity in adults

Seung Pil Bang<sup>1,2</sup>, Ramkumar Sabesan<sup>3</sup> & Geunyoung Yoon<sup>4</sup>✉

We investigated how long-term visual experience with habitual spherical aberration (SA) influences subjective depth of focus (DoF). Nine healthy cycloplegic eyes with habitual SAs of different signs and magnitudes were enrolled. An adaptive optics (AO) visual simulator was used to measure through-focus high-contrast visual acuity after correcting all monochromatic aberrations and imposing  $+0.5\ \mu\text{m}$  and  $-0.5\ \mu\text{m}$  SAs for a 6-mm pupil. The positive ( $n=6$ ) and negative ( $n=3$ ) habitual SA groups ranged from 0.17 to 0.8  $\mu\text{m}$  and from  $-1.2$  to  $-0.12\ \mu\text{m}$  for a 6-mm pupil, respectively. Although all optical conditions were identical, and the subjective DoFs were expected to be the same for all participants, the DoFs of individuals differed between the positive and negative habitual SA groups. For the positive habitual SA group, the mean DoF with positive AO-induced SA (2.14 D) was larger than that with negative AO-induced SA (1.88 D); for the negative habitual SA group, a smaller DoF was measured with positive AO-induced SA (1.94 D) than that with negative AO-induced SA (2.14 D). Subjective DoF tended to be larger when the induced SA in terms of sign and magnitude was closer to the participant's habitual SA. Our findings suggest that neural adaptation to habitual SA compensated for optical blur at multiple object distances, perceptually expanding DoF. As a result, the outcomes of optical treatments for presbyopia may differ due to the neural compensation mechanism influenced by an individual's visual experience with their habitual optics.

**Keywords** Spherical aberration, Neural adaptation, Visual acuity, Adaptive optics, Depth of focus

The ability to objectively assess and understand the habitual primary spherical aberration (SA) of the eye has improved owing to the development of various ocular wavefront sensing techniques<sup>1–3</sup>. SA decreases far image quality but increases the depth of focus (DoF) by primarily affecting defocus. While there is a possibility that SA further interacts with other higher-order aberrations (HOAs), investigating this is challenging due to the significant variation in HOAs between individual eyes. However, the habitual SA is the only HOA with a significantly positive population mean<sup>4,5</sup>. In addition, aging causes progressive alterations in ocular optics, which tends to increase the magnitude of habitual HOAs, especially SA. Moreover, myopic and hyperopic corneal refractive surgeries induce positive and negative SAs, respectively<sup>3,6</sup>. Given that both signs of the induced SA result in multiple focal points formed by rays passing through different pupil areas, inducing SA represents a useful strategy for extending the DoF<sup>7–11</sup>. Instead of correcting the corneal SA in presbyopic patients, aspheric optical designs of intraocular lenses (IOLs) inducing more SAs can provide a continuous focal zone with a small change in point spread function (PSF). Besides conventional spherical IOLs inducing a positive SA<sup>12</sup>, recent extended DoF (EDoF) IOLs based on complex asphericity modulation increase the DoF because of the progressive shift in local power from far to intermediate distance<sup>13–18</sup>.

Interestingly, previous studies have reported the DoF of human eyes with the induced SA, and there were significant variations in DoFs among the studies<sup>9,16,19–24</sup>. As all of these studies were performed with AO correction, this variability cannot be explained by uncorrected residual aberrations. One of the potential reasons for the variability may be the difference in methodology to define the DoF: (1) visibility of the target and (2) degradation of visual acuity (VA) or contrast sensitivity<sup>25</sup>. The former has been widely used;<sup>19–21,26–30</sup> however, it has an intrinsic limitation due to the subjective nature of the blur evaluation<sup>21</sup>. Moreover, the latter is commonly

<sup>1</sup>Department of Ophthalmology, Keimyung University School of Medicine, Daegu, South Korea. <sup>2</sup>Department of Biomedical Engineering, University of Rochester, Rochester, NY, United States. <sup>3</sup>Department of Ophthalmology, University of Washington School of Medicine, Seattle, WA, USA. <sup>4</sup>College of Optometry, University of Houston, Houston, TX 77004, USA. ✉email: gyoon2@central.uh.edu

used based on a resolution threshold<sup>9,16,22,31</sup>. This method may reduce the effect of between-study variability by its objectivity, but variability was still observed within the previous studies.

Within-study variability can be represented by interindividual variability, and individual visual systems can compensate for optical blur via neural adaptation<sup>32</sup>, which involves the strengthening of neural connections<sup>33,34</sup>. This neural compensation is not only limited to defocus blur<sup>35,36</sup>, but also to optical blur induced by HOAs at a single object distance. Recently, Zapata-Diaz et al.<sup>30</sup> expanded the scope further with multiple object distances and demonstrated the significant interindividual variability of the DoF due to neural compensation with the same induced HOA patterns on top of the AO correction of their habitual HOAs. Given that the habitual SA is the only HOA with a significant population distribution, we specifically focused on the habitual SA among HOAs. We hypothesized that subjective DoF extended by the same induced SA depends on a participant's habitual SA due to long-term neural adaptation. It is plausible that long-term exposure to habitual SA modifies the neural processing mechanism to compensate for optical blur at different object distances, resulting in different DoFs under the same optical condition.

To test our hypothesis, the objective of this study was to evaluate the relationship between the increase in subjective DoF caused by induced SAs and habitual SA. To achieve this aim, we induced a fixed magnitude of SA, but with the opposite sign to the eye, using an AO visual simulator to assess the DoF based on the through-focus VA measurement. Our results suggest the significance of customized presbyopia correction for short-term performance. However, there is still a possibility that the visual system may gradually readapt to the new optics over time, leading to an increase in DoF.

## Methods

### Ethics statements

Written informed consent was obtained from all participants, and study approval was obtained from the University of Rochester Research Review Board. This study adhered to the tenets of the Declaration of Helsinki and was conducted in accordance with the United States Health Insurance Portability and Accountability Act.

### Participants

Nine healthy participants (9 eyes in total) participated in this study. All eyes underwent a recent dilated ophthalmological examination, and no pathology was identified in the normal eyes. Participants with spherical equivalent refractions of more than 1.5 diopters (D) or less than  $-1.5$  D, astigmatism of more than 0.75 D, or distance best corrected VA worse than 20/20 were excluded to avoid significant adaptation to defocus, directional blur, and ocular pathology affecting their vision. Participants with previous ocular surgeries (except for corneal refractive surgeries), dry eye, amblyopia, variable pupil sizes, or a history of contact lens use were also excluded. All participants did not have habitual refractive correction. Both 1% tropicamide and 2.5% phenylephrine were instilled at least 30 min before measurement to achieve the full cycloplegic effects of the drugs, confirmed when the dilated pupils did not react to light and the retinoscopic reflex did not fluctuate.

### Adaptive optics visual simulator

The AO visual simulator used in this study has been described elsewhere<sup>37</sup>. Briefly, it comprises a large-stroke deformable mirror (Mirao 52D; Imagine Eyes, Orsay, France)<sup>38</sup>, custom-made Shack–Hartmann wavefront sensor, a Badal optometer to determine the subjective best focus of the eye, an artificial pupil to control the pupil size, and a digital light processing (DLP) projector (Sharp PG-M20X; Sharp Corporation, Japan) to display visual stimuli for VA measurements. The AO visual simulator was operated in a closed loop to control participants' wavefront aberrations in real-time (8 Hz). The wavefront-sensing laser beacon was generated using a superluminescent diode with a center wavelength of 840 nm (bandwidth, 40 nm). Head movements were stabilized with a bite bar, and a phoropter was used to compensate for the sphere and cylinder in some participants partially. Then, the AO visual simulator was used to measure and correct participants' monochromatic wavefront aberrations over a 6-mm pupil to an accuracy of less than  $0.06\ \mu\text{m}$  ( $<\lambda/14$ ) as the residual root mean square error and to induce two Zernike primary SA conditions ( $C_4^0 = +0.5$  and  $-0.5\ \mu\text{m}$ ). Thus, every participant was tested under identical optical conditions. Through-focus high-contrast VA was measured, and the AO closed-loop control maintained the optical conditions in real-time. An experimental overview can be found in Supplementary Fig. S1 online.

### Through-focus VA measurement

The psychophysical procedures were fully controlled by a custom-developed computer program using the Visual Psychophysics Toolbox in MATLAB (Mathworks). For each SA condition, each participant subjectively optimized the retinal image quality by adjusting defocus using the Badal optometer in the AO visual simulator. This approach was used because SA is known to cause a significant shift in the best focus. This procedure ensures that distance visual quality is always optimal, and DoF is measured from this optimized point. Through-focus VA was measured at 8 different optical distances ranging from  $-1$  to  $2.5$  D ( $0.5$ -D increments) in a randomized order generated by the computer program. The high-contrast VA measurement was made with a single tumbling letter "E" (four-alternate forced-choice method) on a uniform background with a mean luminance of  $70\ \text{cd}/\text{m}^2$ . A narrowband interference filter transmitting  $633 \pm 5\ \text{nm}$  light was used to yield a monochromatic stimulus to remove the chromatic aberration of the eye. As the AO visual simulator operated at a different wavelength (840 nm) than the visual stimulus (633 nm), each participant subjectively corrected chromatic defocus for their eyes by adjusting the Badal optometer to the position averaged from three trials.

The through-focus VA measurement was initiated by the participant with a keypress. The participant responded to the letter 'E' orientation displayed for 500 ms in one of 4 orientations (0, 90, 180, 270 deg). The response was followed by auditory feedback and an inter-stimulus interval of 500 ms. The letter size varied according to an adaptive staircase method using the QUEST<sup>39</sup> algorithm. Data from 30 trials were obtained

and fitted using a cumulative Weibull function, with the scale and shape parameters of the function kept as free parameters. Visual acuity was defined as the letter size for which 62.5% of the responses were correct. Three measurements were averaged for each optical condition, given as the logarithm of the minimum angle of resolution (logMAR). If the standard deviation of the three measurements was larger than 0.1 logMAR, the session was aborted and reinitiated to avoid any selection bias. Participants were allowed to take breaks during the measurements whenever requested, and the entire task lasted approximately 3 h.

#### Definition of DoF

The through-focus VA lines were obtained by least-squares linear fitting using MATLAB (MathWorks, Natick, MA, USA), which only included VA responses from the distance to near defocus range (Fig. 1). Data at the defocus range beyond infinity (negative D) were used to ensure the best visual acuity at 0 D but were excluded from the fitting process. From the through-focus VA curve, the DoF was defined as the defocus range in D

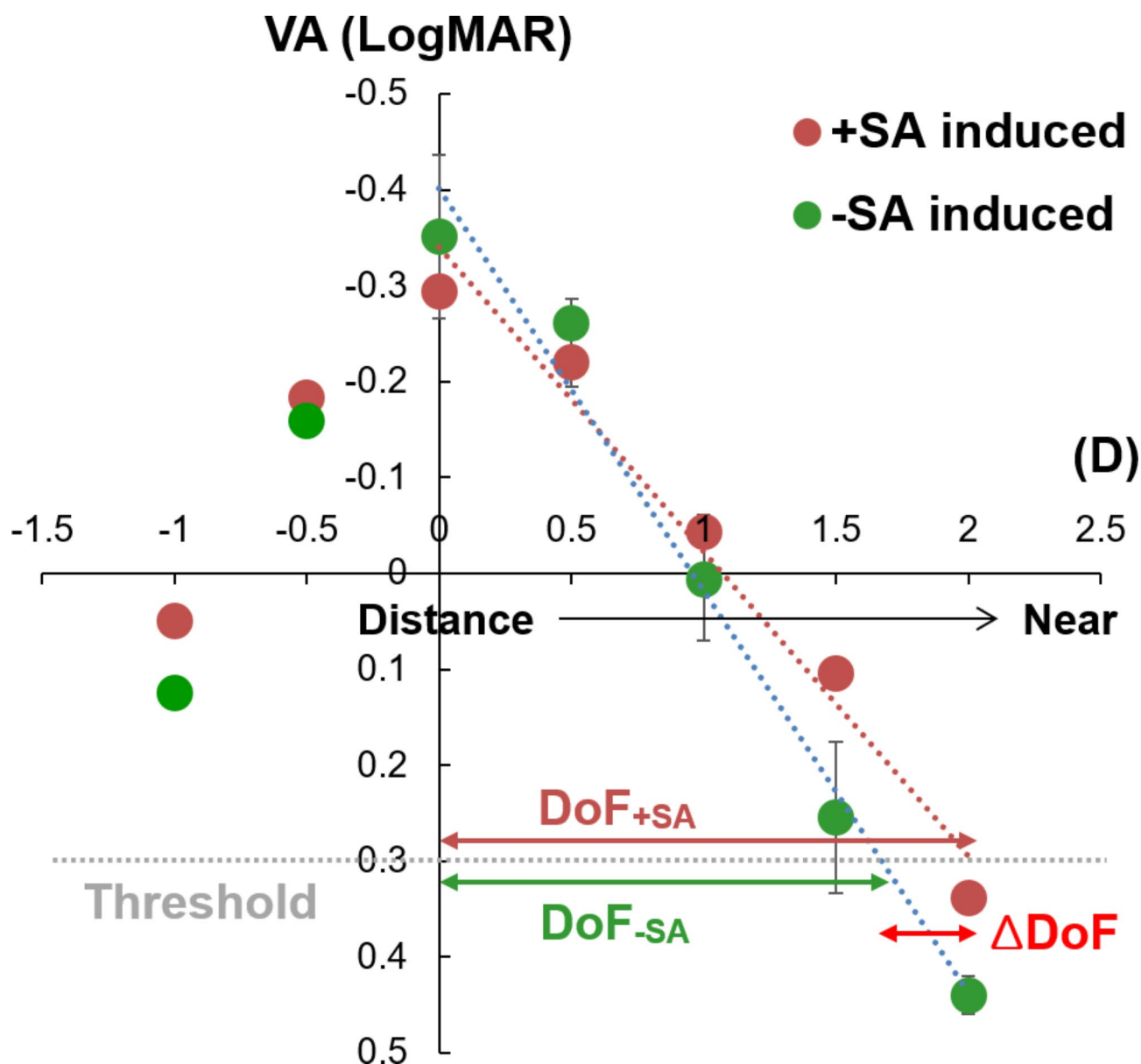


**Fig. 1.** Exemplary through-focus visual acuity (VA) lines from one participant's eye. The through-focus VA lines were obtained by least-squares linear fitting ( $R^2 = 0.97$  for the positive adaptive optics [AO]-induced spherical aberration (SA) condition,  $R^2 = 0.98$  for the negative AO-induced SA condition). The depth of focus (DoF) was defined as the range in diopters (D) from a distance (0 D) to near (positive D) for which acuity surpassed 0.3 logarithm of the minimum angle of resolution or 20/40 on the Snellen acuity scale as a threshold. The difference of DoF ( $\Delta\text{DoF}$ ) between the positive AO-induced SA condition ( $\text{DoF}_{+SA}$ ) and the negative AO-induced SA condition ( $\text{DoF}_{-SA}$ ) was also calculated. Error bars show standard deviations for three repeated measurements.

from distance (0.0 D) to near (positive D), for which acuity is better than 0.3 logMAR or 20/40 on the Snellen acuity scale<sup>40</sup>. We also calculated the difference in the DoF between positive versus negative AO-induced SA ( $\Delta\text{DoF} = \text{DoF}_{+\text{SA}} - \text{DoF}_{-\text{SA}}$ ).

Statistical analysis

This study utilized a small sample size ( $n=9$ ) due to its pilot nature. Previous research<sup>30</sup> has demonstrated significant findings with a similar sample size ( $n=11$ ) in the investigation of DoF and HOAs. Since the Shapiro-Wilk test for normality rejected the null hypothesis that the data follow a normal distribution, non-parametric methods were employed for the statistical analysis. The data are presented as means with 95% confidence intervals (CIs). Effect sizes are also reported to evaluate the magnitude of differences between groups. As there were continuous variables (i.e., DoF) between two categorical independent groups (two AO-induced SA conditions [between-participants factor] and two habitual SA subgroups [within-participants factor]) that were compared, the nparLD R package, developed by Noguchi et al.<sup>41</sup>, was used for the non-parametric mixed-effects model. This package offers researchers an easy and user-friendly way to apply robust rank-based methods for analyzing mixed factorial designs. To validate the nparLD R package, we used sample data to check if we could replicate the results from Noguchi et al.’s study. For post hoc tests in the mixed-effects model, we employed the pairwise Wilcoxon test for pairwise comparisons and the Mann–Whitney U-test for non-pairwise comparisons. Bonferroni correction was applied to adjust for multiple comparisons across subgroups. Given the four comparisons to be conducted, statistical significance was set at  $P$ -values  $< 0.0125$  ( $0.05/4$ ). All analyses were performed using RStudio software (Rstudio Team, Boston, MA, USA).

Results

There were 6 participants with positive SA (age range: 42–57 years, SA range: 0.17–0.8  $\mu\text{m}$  for a 6-mm pupil) and 3 participants with negative SA (age range: 39–59 years, SA range: -1.2 to -0.12  $\mu\text{m}$  for a 6-mm pupil). One participant in the positive SA group underwent myopic corneal refractive surgery, and 2 participants in the negative SA group underwent hyperopic corneal refractive surgery. All 3 participants underwent corneal refractive surgery several years before enrollment (range: 2–4 years). Table 1 summarizes the habitual SAs and DoF values measured under both the positive and negative AO-induced SA conditions for all participants. Generally, a larger DoF was observed in the positive AO-induced SA condition (2.08 D, 95% CI [1.91 D, 2.24 D]) than in the negative AO-induced SA condition (1.97 D, 95% CI [1.80 D, 2.13 D]), but without statistical significance ( $P=0.354$ ) (effect size: 0.43). Additionally, there was no statistically significant difference in the DoF between the positive (2.01 D, 95% CI [1.86 D, 2.16 D]) and negative (2.04 D, 95% CI [1.85 D, 2.24 D]) habitual SA subgroups ( $P=0.779$ ) (effect size: 0.14). The uncorrected interaction effect was large ( $F=0.726$ ,  $P=0.019$ ), however, the main effect of induced SA violated the sphericity assumption. After applying the Greenhouse–Geisser correction, the interaction effect was no longer statistically significant ( $F=0.036$ ,  $P=0.488$ ).

Within the positive habitual SA subgroup, a larger mean DoF was observed with a positive AO-induced SA condition (2.14 D, 95% CI [1.95 D, 2.33 D]) than with a negative AO-induced SA condition (1.88 D, 95% CI [1.69 D, 2.07 D]), but the difference was not statistically significant ( $P=0.075$ ) (effect size: 0.99). This finding might be due to the wide distribution of habitual SA, averaging the effect of the habitual SA on the DoF. Figure 2 shows two extreme examples of through-focus VA lines with different magnitudes of positive habitual SA from 2 participants. In participant 5, with the closest magnitude of habitual SA (+0.55  $\mu\text{m}$ ) to that of AO-induced SA (+0.5  $\mu\text{m}$ ), a larger  $\Delta\text{DoF}$  (0.67 D) was observed compared to participant 1 (-0.11 D), who had the largest difference in magnitude of habitual SA (+0.17  $\mu\text{m}$ ) compared to that of AO-induced SA. The  $\Delta\text{DoF}$  values for

Participant	Habitual SA ( $\mu\text{m}$ )	DoF (D)		Difference ( $\Delta\text{DoF}$ , D)
		+SA induced	-SA induced	
P1	0.17	1.75	1.86	- 0.11
P2	0.20	2.14	1.96	0.18
P3	0.28	2.02	1.68	0.34
P4	0.40	2.46	1.98	0.48
P5	0.55	2.23	1.56	0.67
PS6	0.80	2.24	2.23	0.01
Mean (95% CI)		2.14 (1.95, 2.33)	1.88 (1.69, 2.07)	Effect size: 0.99
P7	- 0.12	2.25	2.40	- 0.15
PS8	- 0.75	1.78	2.09	- 0.31
PS9	- 1.20	1.81	1.94	- 0.13
Mean (95% CI)		1.94 (1.65, 2.24)	2.14 (1.88, 2.41)	Effect size: 0.80
Total mean (95% CI)		2.08 (1.91, 2.24)	1.97 (1.80, 2.13)	Effect size: 0.43

**Table 1.** Summary of the depth of focus (DoF) measurements in both positive and negative adaptive optics (AO)-induced spherical aberrations (SAs) with a broad spectrum of habitual SAs. Data are averages of three measurements. *CI* confidence interval, *D* diopters, *P* participant, *PS* participant with corneal refractive surgery.

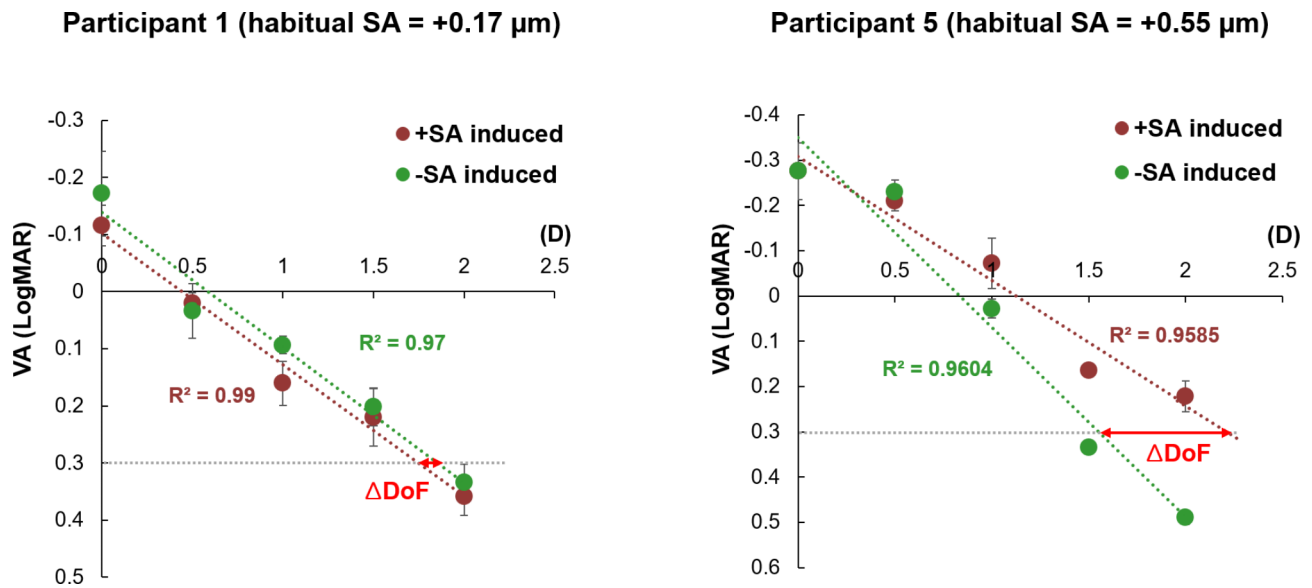


**Fig. 2.** Through-focus visual acuity (VA) lines with different magnitudes of positive habitual spherical aberration (SA). Participant 1 had the most distinct magnitude of habitual SA, while participant 5 had the most comparable magnitude to that of the adaptive optics-induced SA. The through-focus VA lines only included VA responses from the distance to near defocus range. *D* diopters, *DoF* depth of focus.

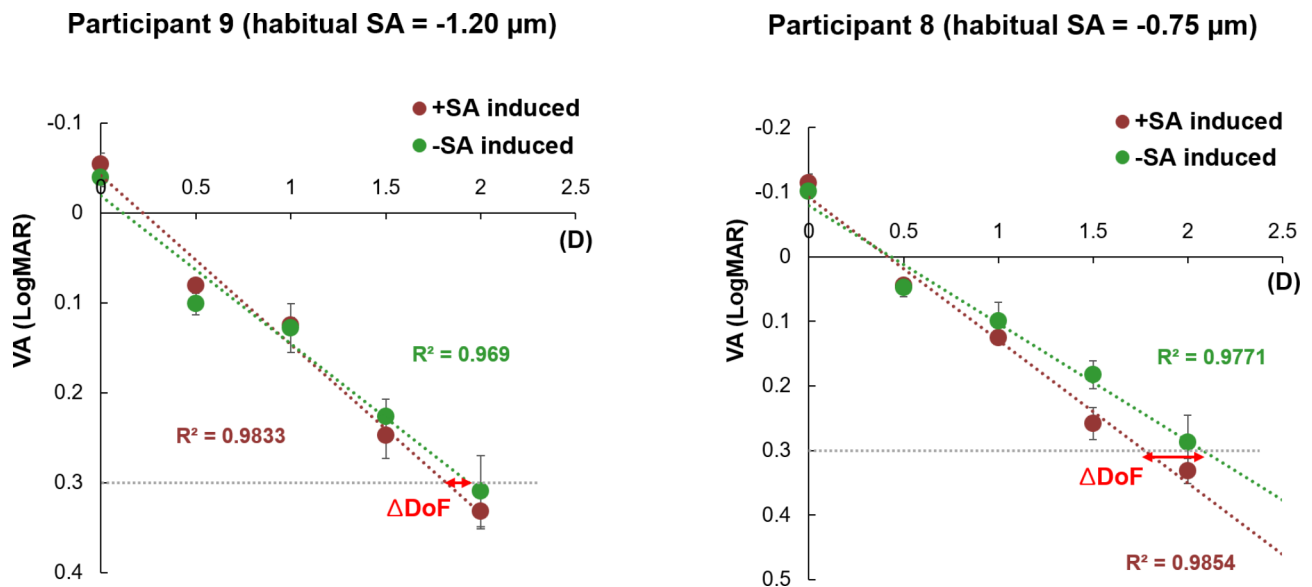


**Fig. 3.** Through-focus visual acuity (VA) lines with different magnitudes of negative habitual spherical aberration (SA). Participant 9 had the most distinct magnitude of habitual SA, while participant 8 had the most comparable magnitude to that of the adaptive optics-induced SA. The through-focus VA lines only included VA responses from the distance to near defocus range. *D* diopters, *DoF* depth of focus.

participants 2, 3, 4, and 6 were 0.18, 0.34, 0.48, and 0.01 D, respectively, all of which were larger than the value from participant 1 but smaller than that from participant 5.

Similarly, within the negative habitual SA subgroup, a larger mean DoF was observed with negative AO-induced SA (2.14 D, 95% CI [1.88 D, 2.41 D]) compared to positive AO-induced SA (1.94 D, 95% CI [1.65 D, 2.24 D]), without statistical significance ( $P=0.275$ ) (effect size: 0.80). Figure 3 shows the through-focus VA curves with extremely different magnitudes of negative habitual SA for 2 participants. In participant 8, with the closest magnitude of habitual SA ( $-0.75 \mu\text{m}$ ) to that of AO-induced SA ( $-0.5 \mu\text{m}$ ), a smaller  $\Delta\text{DoF}$  ( $-0.31$  D) was observed compared to participant 9 ( $-1.20 \mu\text{m}$ ), who had the largest difference between the magnitude of habitual SA ( $-1.20 \mu\text{m}$ ) from that of AO-induced SA. The  $\Delta\text{DoF}$  value for participant 7 was  $-0.15$  D, which was larger than the value from participant 8 but smaller than that from participant 9.

With the positive AO-induced SA condition, there was no statistically significant difference in the DoF between the positive (2.14 D, 95% CI [1.95 D, 2.33 D]) and negative (1.94 D, 95% CI [1.65 D, 2.24 D]) habitual SA subgroups ( $P=0.606$ ) (effect size: 0.78). With the negative AO-induced SA condition, there was also no statistically significant difference in the DoF between the positive (1.88 D, 95% CI [1.69 D, 2.07 D]) and negative (2.14 D, 95% CI [1.88 D, 2.41 D]) habitual SA subgroups ( $P=0.197$ ) (effect size: 1.03).

Figure 4 shows the distribution of  $\Delta\text{DoF}$  with regard to each participant's habitual SA. The grey dashed horizontal line shows the expected outcome from theoretical simulation, constant throughout different habitual SAs due to the optically identical condition with the AO correction. Interestingly, the positive habitual SA subgroup showed higher  $\Delta\text{DoF}$  when the magnitude of the participant's habitual SA was closer to that of the positive-induced SA. The same trend was observed in the negative habitual SA subgroup with the opposite sign because we defined the  $\Delta\text{DoF}$  as the DoF with positive AO-induced SA minus the DoF with negative AO-induced SA. In other words, a negative  $\Delta\text{DoF}$  indicates that the DoF with a negative AO-induced SA was larger than that with a positive AO-induced SA.

## Discussion

The main objective of this study was to investigate whether habitual SA affects the DoF extended by artificially induced SA. Our results showed that while all optical conditions were identical in all participants with AO-based correction and SA induction, the subjective DoFs differed among individuals. Interestingly, the difference in the DoF between positive and negative AO-induced SA tended to be higher when the magnitude of the participants'

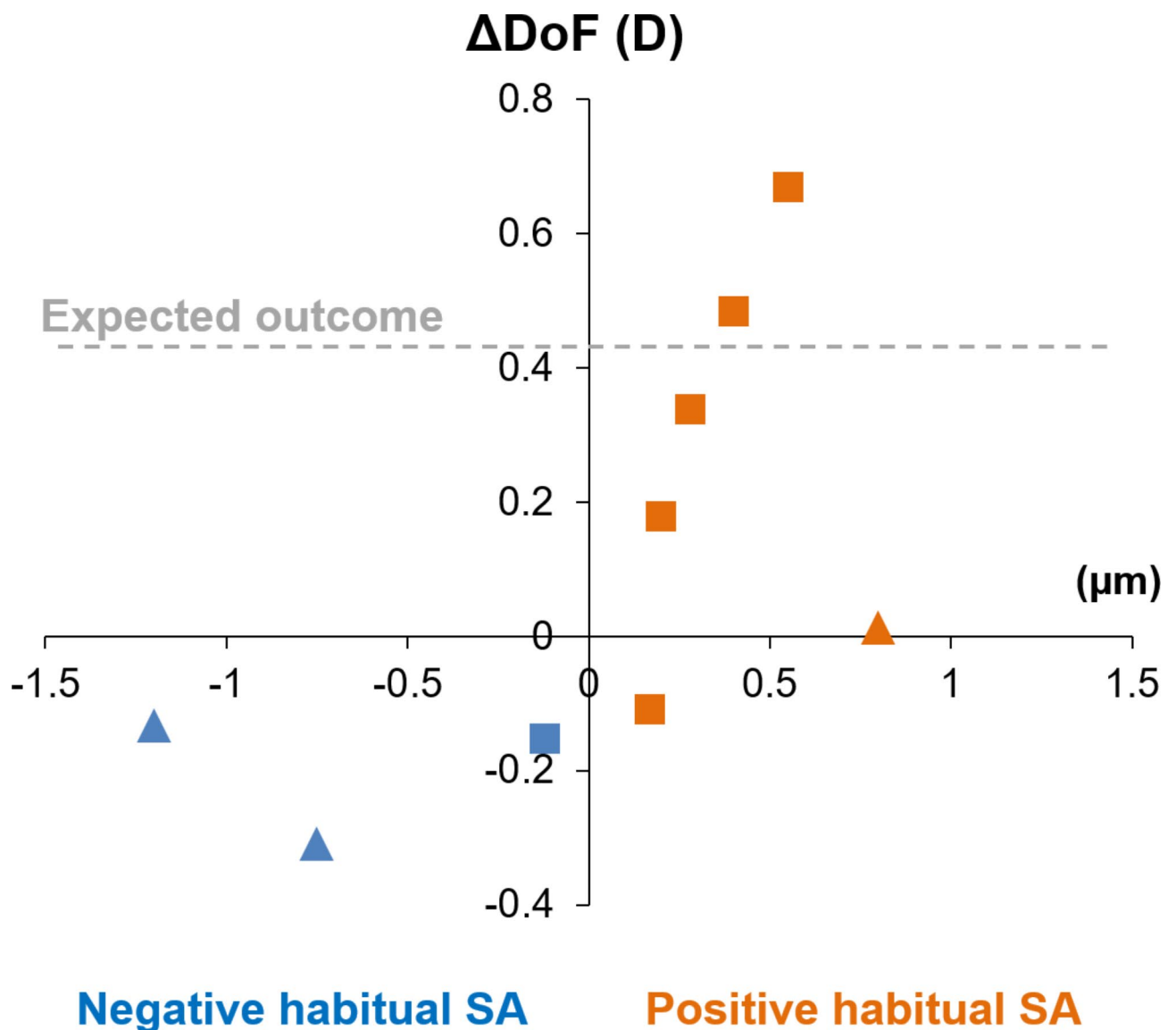


**Fig. 4.** Distribution of the difference in the depth of focus ( $\Delta\text{DoF}$ ) with positive and negative adaptive optics (AO)-induced spherical aberrations (SAs). Triangle symbols: participants with corneal refractive surgery; square symbols: participants with no surgery. *D* diopters.



habitual SA was closer to that of the AO-induced SA. These results suggest that the individual visual system that adapted to the specific sign and magnitude of the habitual SA plays an important role in determining the subjective DoF.

The balance between the retinal image quality and DoF is essential in the design of various optical treatments for presbyopia, such as contact lenses or IOLs. These optical treatments aim to support the presbyope with optimal retinal image quality over a broad range of object distances. Induction of HOAs, rather than correcting them, has been used to extend the through-focus optical quality of the eye. Rotationally asymmetric aberrations, such as coma-like aberrations, can increase the DoF owing to the increased size of the PSF at the expense of reduced retinal image quality<sup>9,42–44</sup>. However, there is insufficient consensus on their effect on the estimated DoF. For instance, Rocha et al.<sup>9</sup> reported that trefoil and coma had no significant impact on the subjective DoF, whereas Legras et al.<sup>42</sup> demonstrated that coma had a significant influence on the DoF. Moreover, asymmetric aberrations themselves significantly negatively influence retinal image quality, which could be the major reason coma or secondary astigmatic aberrations have drawn less attention. Asymmetric aberrations degrade retinal image quality for far vision, but can increase the DoF of the eye<sup>45–47</sup>, thus a trade-off exists between an optimal level of retinal image quality and the DoF<sup>29,48</sup>.

On the other hand, a radially symmetric aberration, SA increases the DoF with less compromise of retinal image quality at optimal focus<sup>7,49</sup>. As aforementioned, SA can extend the DoF of the eye, as it can generate multiple focal points near the retinal plane by rays passing through different pupil areas as a function of the radial distance from the center of the pupil. Figure 5 shows the defocus curves of the positive and negative 0.5  $\mu\text{m}$  SAs used in this study. The y-axis shows the area under the modulation transfer function (MTF), and the DoF can be estimated at the threshold used in our study, 0.3 logMAR, by using the area under the MTF, based on a regression model in previous studies<sup>50–52</sup>. The peaks of the through-focus curves shifted by the induced SAs were corrected to ensure that the retinal image quality was optimal at a far distance (0 D), in accordance with our experimental protocol. Based on the DoF definition in this study, as the defocus ranges from a distance (with the best image quality) to near, a larger DoF was observed with a positive-induced SA condition compared to a negative-induced SA condition in the simulation. However, the result in our study that the negative habitual SA group showed no significant difference in DoF between the positive and negative induced SA conditions cannot be explained by the simulation. This discrepancy in addition to the observed variation in individual subjective DoF under the same SA conditions, indicates that the optical effect is not the sole factor affecting DoF.

AO has been widely used to separate neural factors from optical factors by creating identical optical conditions for individual subjects by correcting dynamically<sup>53</sup> and inducing a certain aberration profile to the eye<sup>54</sup>. Atchison et al.<sup>28</sup> found considerable interindividual variability in noticeable and objectionable blur, even though they corrected all HOAs in their participants, indicating that the neural processing associated with blur detection might vary among participants. Zapata-Diaz et al.<sup>30</sup> paid attention to this interindividual variability and assessed whether habitual HOA alone or neural factors can explain this variability. By swapping participants' habitual HOAs with each other, they observed that inducing new HOA patterns tended to reduce the DoF in most participants and that the effect of neural adaptation on the interindividual variability of DoF with the new optics was significantly greater than that with their habitual HOAs. Previous studies<sup>9,22</sup> have reported the inter-subject variability of the DoF with the identical optical condition (AO-induced SA + habitual aberration

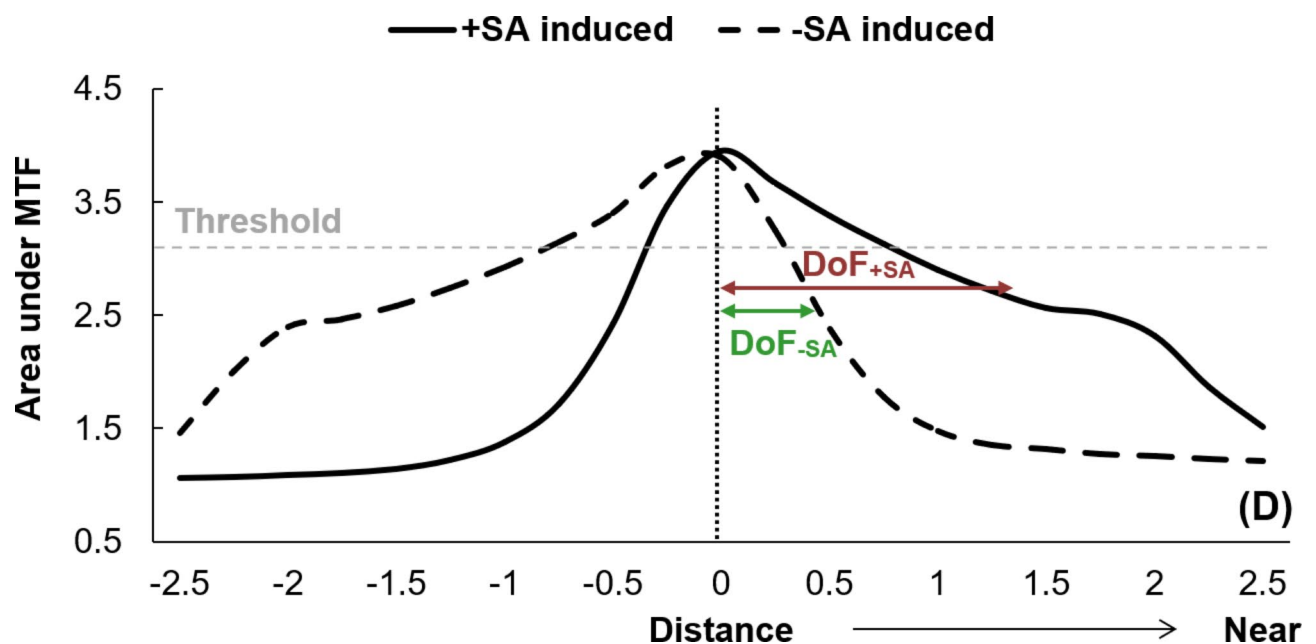


**Fig. 5.** Theoretical estimation of the depth of focus with the positive adaptive optics (AO)-induced spherical aberration (SA) condition ( $\text{DoF}_{+SA}$ ) versus the negative AO-induced SA condition ( $\text{DoF}_{-SA}$ ).  $D$  diopters, MTF modulation transfer function.

correction) among individuals, however, the potential correlation between the finding and habitual SA has not been studied. A recent study<sup>16</sup> presented the interindividual variability of the DoF with the same optical condition (SA-based EDoF IOL profile + habitual aberration correction). The authors did not find a tendency associated with the magnitude of the habitual SAs, but the magnitude of the habitual SAs was small without confounding factors such as cataract<sup>55</sup> or dry eye<sup>56</sup>. These previous studies involved much narrower ranges of participants' habitual SA (ranges [ $\mu\text{m}$ ]:  $-0.07$ – $0.23$ <sup>9</sup> and  $-0.13$ – $0.38$ <sup>22</sup> with a 6-mm pupil and  $0$ – $0.14$ <sup>16</sup> with a 4.5-mm pupil) compared to ours (range:  $-1.20$ – $0.80$   $\mu\text{m}$  with a 6-mm pupil).

How does habitual SA affect the DoF induced by SA? Contrast perception by the human visual system is established with multiple spatial frequency-specific channels in the visual cortex<sup>57</sup>. These channels can adjust contrast gains in response to changes in the visual environment. Georgeson and Sullivan<sup>58</sup> proposed that a continuous feedback mechanism in the visual system could compensate for the attenuated contrast by the ocular optics to maintain perceived contrast constant across a wide spatial frequency range as long as retinal contrast is above the threshold, i.e., contrast constancy<sup>36</sup>. Furthermore, the human neural system is capable of compensating for optical blur induced by defocus<sup>35,36</sup>. Subsequent studies have reported that the neural system of healthy eyes, exhibiting typical optical quality<sup>59,60</sup>, as well as those with severe optical abnormalities<sup>61,62</sup>, can also compensate for habitual optical blur induced by HOAs after both short-<sup>63</sup> and long-term exposure<sup>62,64</sup> to aberrated stimuli. We have recently proposed an additional neural compensation mechanism, the partial restoration of phase congruency by altering phase perception for habitual optical blur<sup>65,66</sup>. These neural compensatory mechanisms may explain our extended findings involving adjusting contrast gain and phase relationships of various spatial frequencies. Adaptation might occur based on the entire aberration pattern (or blur) rather than individual aberration modes, each having distinct impacts on contrast and phase shift at different spatial frequencies. In the context of the present study, SA could be the aberration that contributes most to adaptation, given its magnitude is much larger than other HOAs. This does not negate the potential contribution of other HOAs, but we speculate that their impact would be relatively smaller than SA, especially in individuals with large habitual SA. Moreover, prolonged visual experience with a certain sign and magnitude of habitual SA combined with various magnitudes of defocus (i.e., from far to near vision) may allow the neural system to compensate for blur under multiple optical states<sup>67</sup>. This provides important insights into the capacity of the presbyope's neural system to deblur not only for a single distance but also for a range of target vergences.

In Fig. 4, the positive and negative habitual SA groups showed different magnitudes of  $\Delta\text{DoF}$ . This result may be due to interindividual differences in the exposure period to chronic blur. Participants who underwent corneal refractive surgery had much shorter adaptation periods (PS6: 4 years, PS8: 2 years, and PS9: 3 years) than those with normal optics. In some of these participants, the neural adaptation process may still be in progress. This might mean that a larger blur compensation could be gained later as they experience their "habitual" SA longer, resulting in a larger DoF, especially for the negative habitual SA group, where two of the three participants underwent corneal refractive surgery. However, there is clinical evidence regarding the timescale for neural adaptation to enhanced optical quality following corneal refractive surgery. Pesudovs<sup>68</sup> focused on visual acuity changes over shorter time intervals post-LASIK, reporting that the neural system typically requires approximately 10 weeks to adapt to a new state of blur following refractive surgery. This duration is notably shorter than the adaptation periods covered in our study. However, these differing adaptation periods to habitual SA (2–4 years for refractive surgery versus lifelong for healthy participants) could have influenced the results. Furthermore, refractive surgery might introduce additional ocular wavefront changes besides SA that could impact visual performance. Further investigations are required to support this explanation.

These findings have important clinical implications. Presbyopia-correcting IOLs have been designed to have different SAs and individual patients also have diverse magnitudes of corneal SA; therefore, the consequent total SA after cataract surgery will vary in terms of the sign and magnitude. This variation in the ocular SA could affect the subjective DoF, even if some IOLs are not specifically designed to extend the DoF with SA modulation. The neural compensatory mechanism evoked by individual habitual SA could also affect the subjective DoF, at least in the short term after surgery. Moreover, given that neural plasticity seems to exist in aged pseudophakic eyes<sup>69</sup>, the aging visual system may be capable of re-adapting to new optics (i.e., IOLs) over time, resulting in increasing DoF. It would be intriguing to examine the extent to which plasticity improves subjective DoF with presbyopia-correcting optical/surgical treatments.

A major limitation of our study was the small sample size ( $n=9$ ). Since we sought to recruit participants with a wide range of habitual SAs, obtaining a larger sample size for statistical power was challenging. Finding participants with a substantial magnitude of SAs and no history of corneal refractive surgeries also proved challenging. According to the sample size calculation derived from our results, a minimum of 15 participants for each habitual SA group is necessary, and a future study with sufficient statistical power may support our proposed adaptive mechanisms more robustly. Furthermore, if chromatic stimuli resembling natural scenes were employed, the subjective DoF might differ due to the presence of longitudinal chromatic aberration. Additionally, the timing and integration of various systems, as in the accommodative control system, are important factors to consider in neural adaptation at different vergence levels. On the other hand, the impact of the Stiles–Crawford effect (SCE) combined with SA on DoF was not considered in our study. It has been reported that both the SCE and SA increased DoF, and the SCE improved image quality in an aberrated eye with SA only when defocus and SA have the same sign<sup>70</sup>. Another study reported that the SCE had a small compensating capability for SA (and defocus)<sup>71</sup>. Moreover, it is crucial to note that the influence of the SCE on DoF with higher magnitudes of SA in our study ( $0.5$   $\mu\text{m}$  in 6 mm pupil) could differ from that in previous literature ( $0.2$   $\mu\text{m}$  in 6 mm pupil), and there might be interindividual variation in the SCE. In addition, although participants had a practice session to familiarize themselves with the experimental tasks before the data collection, there might have been short-term adaptation to artificially induced blur that might have affected the subjective DoF<sup>72</sup>. However, short-term



blur adaptation was also reported to be limited after the first 6 min<sup>73</sup>. Therefore, this effect would have been insignificant after the practice session in our study.

Herein, we used AO to correct all monochromatic aberrations and examined the visual response to induced SA to determine whether habitual SA can influence the subjective DoF. Our findings suggested that neural adaptation to habitual SA compensated for the optical blur from far to near vision perceptually, resulting in extending the DoF. Therefore, the outcomes of optical treatments for presbyopia could vary due to the neural compensatory mechanism based on their habitual optics.

## Data availability

The datasets used and/or analysed during the current study are available from the corresponding author on reasonable request.

Received: 1 February 2024; Accepted: 3 October 2024

Published online: 05 November 2024

## References

- Thibos, L. N. & Hong, X. Clinical applications of the Shack-Hartmann aberrometer. *Optom. Vis. Sci.* **76**, 817–825. <https://doi.org/10.1097/00006324-199912000-00016> (1999).
- Artal, P., Guirao, A., Berrio, E. & Williams, D. R. Compensation of corneal aberrations by the internal optics in the human eye. *J. Vis.* **1**, 1–8. <https://doi.org/10.1167/1.1.1> (2001).
- Yoon, G., Macrae, S., Williams, D. R. & Cox, I. G. Causes of spherical aberration induced by laser refractive surgery. *J. Cataract Refract. Surg.* **31**, 127–135. <https://doi.org/10.1016/j.jcrs.2004.10.046> (2005).
- Williams, D. et al. Visual benefit of correcting higher order aberrations of the eye. *J. Refract. Surg.* **16**, 554–559. <https://doi.org/10.3928/1081-597X-20000901-12> (2000).
- Porter, J., Guirao, A., Cox, I. G. & Williams, D. R. Monochromatic aberrations of the human eye in a large population. *J. Opt. Soc. Am. Opt. Image Sci. Vis.* **18**, 1793–1803. <https://doi.org/10.1364/josaa.18.001793> (2001).
- Leray, B. et al. Relationship between Induced Spherical aberration and depth of Focus after Hyperopic LASIK in Presbyopic patients. *Ophthalmology*. **122**, 233–243. <https://doi.org/10.1016/j.ophtha.2014.08.021> (2015).
- Nio, Y. K. et al. Spherical and irregular aberrations are important for the optimal performance of the human eye. *Ophthalmic Physiol. Opt.* **22**, 103–112. <https://doi.org/10.1046/j.1475-1313.2002.00019.x> (2002).
- Cheng, H. et al. A population study on changes in wave aberrations with accommodation. *J. Vis.* **4**, 272–280. <https://doi.org/10.1167/4.4.3> (2004).
- Rocha, K. M., Vabre, L., Chateau, N. & Krueger, R. R. Expanding depth of focus by modifying higher-order aberrations induced by an adaptive optics visual simulator. *J. Cataract Refract. Surg.* **35**, 1885–1892. <https://doi.org/10.1016/j.jcrs.2009.05.059> (2009).
- Villegas, E. A. et al. Extended depth of Focus with Induced Spherical Aberration in Light-Adjustable intraocular lenses. *Am. J. Ophthalmol.* **157**, 142–149. <https://doi.org/10.1016/j.ajo.2013.08.009> (2014).
- Xu, R., Wang, H., Jaskulski, M., Kollbaum, P. & Bradley, A. Small-pupil versus multifocal strategies for expanding depth of focus of presbyopic eyes. *J. Cataract Refract. Surg.* **45**, 647–655. <https://doi.org/10.1016/j.jcrs.2019.01.015> (2019).
- Alarcon, A. et al. Optical bench evaluation of the effect of pupil size in new generation monofocal intraocular lenses. *BMC Ophthalmol.* **23**. <https://doi.org/10.1186/s12886-023-02839-y> (2023).
- Rampat, R. & Gatineau, D. Multifocal and extended depth-of-focus intraocular lenses in 2020. *Ophthalmology*. **128**, e164–e185. <https://doi.org/10.1016/j.ophtha.2020.09.026> (2021).
- Labuz, G. et al. Laboratory Investigation of preclinical visual-quality metrics and halo-size in enhanced monofocal intraocular lenses. *Ophthalmol. Ther.* **10**, 1093–1104. <https://doi.org/10.1007/s40123-021-00411-9> (2021).
- Schmid, R. & Borkenstein, A. F. Analysis of higher order aberrations in recently developed wavefront-shaped IOLs. *Graefes Arch. Clin. Exp. Ophthalmol.* **260**, 609–620. <https://doi.org/10.1007/s00417-021-05362-2> (2022).
- Lago, C. M., de Castro, A., Benedi-Garcia, C., Aissati, S. & Marcos, S. Evaluating the effect of ocular aberrations on the simulated performance of a new refractive IOL design using adaptive optics. *Biomed. Opt. Express*. **13**, 6682–6694. <https://doi.org/10.1364/BIOE.473573> (2022).
- Azor, J. A., Vega, F., Armengol, J. & Millan, M. S. Optical assessment and expected visual quality of four extended range of vision intraocular lenses. *J. Refract. Surg.* **38**, 688–697. <https://doi.org/10.3928/1081597X-20220926-01> (2022).
- Megiddo-Barnir, E. & Alio, J. L. Latest development in extended depth-of-focus intraocular lenses: an update. *Asia Pac. J. Ophthalmol. (Phila)*. **12**, 58–79. <https://doi.org/10.1097/APO.0000000000000590> (2023).
- Benard, Y., Lopez-Gil, N. & Legras, R. Subjective depth of field in presence of 4th-order and 6th-order Zernike spherical aberration using adaptive optics technology. *J. Cataract Refract. Surg.* **36**, 2129–2138. <https://doi.org/10.1016/j.jcrs.2010.07.022> (2010).
- Benard, Y., Lopez-Gil, N. & Legras, R. Optimizing the subjective depth-of-focus with combinations of fourth- and sixth-order spherical aberration. *Vision. Res.* **51**, 2471–2477. <https://doi.org/10.1016/j.visres.2011.10.003> (2011).
- Yi, F., Iskander, D. R. & Collins, M. Depth of focus and visual acuity with primary and secondary spherical aberration. *Vis. Res.* **51**, 1648–1658. <https://doi.org/10.1016/j.visres.2011.05.006> (2011).
- Hervella, L., Villegas, E. A., Robles, C. & Artal, P. Spherical Aberration Customization to extend the depth of Focus with a clinical adaptive Optics Visual Simulator. *J. Refract. Surg.* **36**, 223–229. <https://doi.org/10.3928/1081597X-20200212-02> (2020).
- Piers, P. A., Manzanera, S., Prieto, P. M., Gorceix, N. & Artal, P. Use of adaptive optics to determine the optimal ocular spherical aberration. *J. Cataract Refract. Surg.* **33**, 1721–1726. <https://doi.org/10.1016/j.jcrs.2007.08.001> (2007).
- Manzanera, S. & Artal, P. Minimum change in spherical aberration that can be perceived. *Biomed. Opt. Express*. **7**, 3471–3477. <https://doi.org/10.1364/Boe.7.003471> (2016).
- Wang, B. & Ciuffreda, K. J. Depth-of-focus of the human eye: theory and clinical implications. *Surv. Ophthalmol.* **51**, 75–85. <https://doi.org/10.1016/j.survophthal.2005.11.003> (2006).
- Tucker, J. & Charman, W. N. The depth-of-focus of the human eye for Snellen letters. *Am. J. Optom. Physiol. Opt.* **52**, 3–21. <https://doi.org/10.1097/00006324-197501000-00002> (1975).
- Atchison, D. A., Fisher, S. W., Pedersen, C. A. & Ridall, P. G. Noticeable, troublesome and objectionable limits of blur. *Vis. Res.* **45**, 1967–1974. <https://doi.org/10.1016/j.visres.2005.01.022> (2005).
- Atchison, D. A., Guo, H. & Fisher, S. W. Limits of spherical blur determined with an adaptive optics mirror. *Ophthalmic Physiol. Opt.* **29**, 300–311. <https://doi.org/10.1111/j.1475-1313.2009.00637.x> (2009).
- Yi, F., Iskander, D. R. & Collins, M. J. Estimation of the depth of focus from wavefront measurements. *J. Vis.* **10** (3 1–9). <https://doi.org/10.1167/10.4.3> (2010).
- Zapata-Diaz, J. F., Marin-Franch, I. & Radhakrishnan, H. Lopez-Gil, N. Impact of higher-order aberrations on depth-of-field. *J. Vis.* **18**. <https://doi.org/10.1167/18.12.5> (2018).

31. Zheleznyak, L., Sabesan, R., Oh, J. S., MacRae, S. & Yoon, G. Modified monovision with spherical aberration to improve presbyopic through-focus visual performance. *Invest. Ophthalmol. Vis. Sci.* **54**, 3157–3165. <https://doi.org/10.1167/iovs.12-11050> (2013).
32. Webster, M. A. Visual adaptation. *Annu. Rev. Vis. Sci.* **1**, 547–567. <https://doi.org/10.1146/annurev-vision-082114-035509> (2015).
33. Usrey, W. M., Reppas, J. B. & Reid, R. C. Specificity and strength of retinogeniculate connections. *J. Neurophysiol.* **82**, 3527–3540. <https://doi.org/10.1152/jn.1999.82.6.3527> (1999).
34. Kurzawski, J. W., Mikellidou, K., Morrone, M. C. & Pestilli, F. The visual white matter connecting human area prostriata and the thalamus is retinotopically organized. *Brain Struct. Function.* **225**, 1839–1853. <https://doi.org/10.1007/s00429-020-02096-5> (2020).
35. Mon-Williams, M., Tresilian, J. R., Strang, N. C., Kochhar, P. & Wann, J. P. Improving vision: neural compensation for optical defocus. *Proc. Biol. Sci.* **265**, 71–77. <https://doi.org/10.1098/rspb.1998.0266> (1998).
36. Webster, M. A., Georgeson, M. A. & Webster, S. M. Neural adjustments to image blur. *Nat. Neurosci.* **5**, 839–840. <https://doi.org/10.1038/nn906> (2002).
37. Sabesan, R., Ahmad, K. & Yoon, G. Correcting highly aberrated eyes using large-stroke adaptive optics. *J. Refract. Surg.* **23**, 947–952. <https://doi.org/10.3928/1081-597X-20071101-16> (2007).
38. Fernandez, E. J. et al. Adaptive optics with a magnetic deformable mirror: applications in the human eye. *Opt. Express.* **14**, 8900–8917. <https://doi.org/10.1364/oe.14.008900> (2006).
39. Watson, A. B. & Pelli, D. G. QUEST: a bayesian adaptive psychometric method. *Percept. Psychophys.* **33**, 113–120. <https://doi.org/10.3758/bf03202828> (1983).
40. Plakitsi, A. & Charman, W. N. Comparison of the depths of focus with the naked eye and with three types of presbyopic contact lens correction. *J. Br. Contact Lens Assoc.* **18**, 119–125. [https://doi.org/10.1016/S0141-7037\(95\)80023-9](https://doi.org/10.1016/S0141-7037(95)80023-9) (1995).
41. Noguchi, K., Gel, Y. R., Brunner, E., Konietzschke, F. & nparLD An R Software Package for the Nonparametric Analysis of Longitudinal Data in Factorial experiments. *J. Stat. Softw.* **50**, 1–23. <https://doi.org/10.18637/jss.v050.i12> (2012).
42. Legras, R., Benard, Y. & Lopez-Gil, N. Effect of coma and spherical aberration on depth-of-focus measured using adaptive optics and computationally blurred images. *J. Cataract Refract. Surg.* **38**, 458–469. <https://doi.org/10.1016/j.jcrs.2011.10.032> (2012).
43. Marcos, S. et al. Impact of astigmatism and high-order aberrations on subjective best focus. *J. Vis.* **15**, 4. <https://doi.org/10.1167/15.11.4> (2015).
44. Aguila-Carrasco, A. J., Read, S. A., Montes-Mico, R. & Iskander, D. R. The effect of aberrations on objectively assessed image quality and depth of focus. *J. Vis.* **17**. <https://doi.org/10.1167/17.2.2> (2017).
45. Artal, P., Celestino Marcos, S., Fonolla Navarro, R., Miranda, I. & Ferro, M. Through focus image quality of eyes implanted with monofocal and multifocal intraocular lenses. *Opt. Eng.* **34** (1995).
46. Schwiagerling, J. Analysis of the optical performance of presbyopia treatments with the defocus transfer function. *J. Refract. Surg.* **23**, 965–971. <https://doi.org/10.3928/1081-597X-20071101-19> (2007).
47. Ramos-Lopez, D., Martinez-Finkelshtein, A. & Iskander, D. R. Computational aspects of the through-focus characteristics of the human eye. *J. Opt. Soc. Am. Opt. Image Sci. Vis.* **31**, 1408–1415. <https://doi.org/10.1364/JOSAA.31.001408> (2014).
48. Marcos, S., Moreno, E. & Navarro, R. The depth-of-field of the human eye from objective and subjective measurements. *Vis. Res.* **39**, 2039–2049. [https://doi.org/10.1016/S0042-6989\(98\)00317-4](https://doi.org/10.1016/S0042-6989(98)00317-4) (1999).
49. Jansoni, N. M. & Kooijman, A. C. The effect of spherical and other aberrations upon the modulation transfer of the defocused human eye. *Ophthalmic Physiol. Opt.* **18**, 504–513 (1998).
50. Alarcon, A. et al. Preclinical metrics to predict through-focus visual acuity for pseudophakic patients. *Biomed. Opt. Express.* **7**, 1877–1888. <https://doi.org/10.1364/BOE.7.001877> (2016).
51. Vega, F. et al. Visual acuity of pseudophakic patients predicted from in-vitro measurements of intraocular lenses with different design. *Biomed. Opt. Express.* **9**, 4893–4906. <https://doi.org/10.1364/BOE.9.004893> (2018).
52. Labuz, G., Yan, W., Khoramnia, R. & Auffarth, G. U. Optical-quality analysis and defocus-curve simulations of a novel hydrophobic trifocal intraocular lens. *Clin. Ophthalmol.* **17**, 3915–3923. <https://doi.org/10.2147/OPTH.S445461> (2023).
53. Wu, Y. C., Chang, J. C. & Chang, C. Y. Adaptive optics for dynamic aberration compensation using parallel model-based controllers based on a field programmable gate array. *Opt. Express.* **29**, 21129–21142. <https://doi.org/10.1364/OE.428247> (2021).
54. Hickenbotham, A., Tiruveedhula, P. & Roorda, A. Comparison of spherical aberration and small-pupil profiles in improving depth of focus for presbyopic corrections. *J. Cataract Refract. Surg.* **38**, 2071–2079. <https://doi.org/10.1016/j.jcrs.2012.07.028> (2012).
55. Rajagopalan, A. S., Shahidi, M., Alexander, K. R., Fishman, G. A. & Zelkha, R. Higher-order wavefront aberrations in retinitis pigmentosa. *Optom. Vis. Sci.* **82**, 623–628. <https://doi.org/10.1097/01.opx.0000171335.57812.a2> (2005).
56. Rhee, J. et al. A systematic review on the association between tear film metrics and higher order aberrations in dry eye disease and treatment. *Ophthalmol. Therapy.* **11**, 35–67. <https://doi.org/10.1007/s40123-021-00419-1> (2022).
57. Blakemore, C. & Campbell, F. W. On the existence of neurones in the human visual system selectively sensitive to the orientation and size of retinal images. *J. Physiol.* **203**, 237–260. <https://doi.org/10.1113/jphysiol.1969.sp008862> (1969).
58. Georgeson, M. A. & Sullivan, G. D. Contrast constancy: deblurring in human vision by spatial frequency channels. *J. Physiol.* **252**, 627–656. <https://doi.org/10.1113/jphysiol.1975.sp011162> (1975).
59. Artal, P. et al. Neural compensation for the eye's optical aberrations. *J. Vis.* **4**, 281–287. <https://doi.org/10.1167/4.4.4> (2004).
60. Chen, L., Artal, P., Gutierrez, D. & Williams, D. R. Neural compensation for the best aberration correction. *J. Vis.* **7**. <https://doi.org/10.1167/7.10.9> (2007).
61. Sabesan, R. & Yoon, G. Visual performance after correcting higher order aberrations in keratoconic eyes. *J. Vis.* **9**, 6 1–10. <https://doi.org/10.1167/9.5.6> (2009).
62. Sabesan, R. & Yoon, G. Neural compensation for long-term asymmetric optical blur to improve visual performance in keratoconic eyes. *Invest. Ophthalmol. Vis. Sci.* **51**, 3835–3839. <https://doi.org/10.1167/iovs.09-4558> (2010).
63. Sawides, L., de Gracia, P., Dorronsoro, C., Webster, M. & Marcos, S. Adapting to blur produced by ocular high-order aberrations. *J. Vis.* **11**. <https://doi.org/10.1167/11.7.21> (2011).
64. Barbot, A. et al. Functional reallocation of sensory processing resources caused by long-term neural adaptation to altered optics. *Elife.* **10**. <https://doi.org/10.7554/eLife.58734> (2021).
65. Barbot, A. et al. Improved phase processing following long-term adaptation to optical aberrations in keratoconus. *Invest. Ophthalmol. Vis. Sci.* **56**, 3569–3569 (2015).
66. Yoon, G., Ng, C. J., Tadin, D., Blake, R. & Banks, M. S. Phase perception altered by long-term neural adaptation to habitual optics reduces neural binocular summation. *Invest. Ophthalmol. Vis. Sci.* **60**, 606–606 (2019).
67. Ng, C. J., Sabesan, R., Barbot, A., Banks, M. S. & Yoon, G. Suprathreshold contrast perception is altered by long-term adaptation to Habitual Optical Blur. *Invest. Ophthalmol. Vis. Sci.* **63**, 6. <https://doi.org/10.1167/iovs.63.11.6> (2022).
68. Pesudovs, K. Involvement of neural adaptation in the recovery of vision after laser refractive surgery. *J. Refract. Surg.* **21**, 144–147. <https://doi.org/10.3928/1081-597X-20050301-08> (2005).
69. Bang, S. P., Aaker, J. D., Sabesan, R. & Yoon, G. Improvement of neural contrast sensitivity after long-term adaptation in pseudophakic eyes. *Biomed. Opt. Express.* **13**, 4528–4538. <https://doi.org/10.1364/BOE.465117> (2022).
70. Zhang, X. X., Ye, M., Bradley, A. & Thibos, L. Apodization by the Stiles-Crawford effect moderates the visual impact of retinal image Defocus. *J. Opt. Soc. Am. a-Optics Image Sci. Vis.* **16**, 812–820. <https://doi.org/10.1364/Josaa.16.000812> (1999).
71. Atchison, D. A., Joblin, A. & Smith, G. Influence of Stiles-Crawford effect apodization on spatial visual performance. *J. Opt. Soc. Am. a-Optics Image Sci. Vis.* **15**, 2545–2551. <https://doi.org/10.1364/Josaa.15.002545> (1998).
72. Cufflin, M. P., Mankowska, A. & Mallen, E. A. Effect of blur adaptation on blur sensitivity and discrimination in emmetropes and myopes. *Invest. Ophthalmol. Vis. Sci.* **48**, 2932–2939. <https://doi.org/10.1167/iovs.06-0836> (2007).

73. Khan, K. A., Dawson, K., Mankowska, A., Cufflin, M. P. & Mallen, E. A. The time course of blur adaptation in emmetropes and myopes. *Ophthalmic Physiol. Opt.* **33**, 305–310. <https://doi.org/10.1111/opo.12031> (2013).

## Acknowledgements

This study was conducted at the University of Rochester Flaum Eye Institute.

## Author contributions

G.Y. designed and directed research; R.S. acquired data; S.P.B., R.S., and G.Y. analyzed and interpreted data; S.P.B. wrote the paper; and S.P.B. and G.Y. provided critical revision of the manuscript for intellectual content.

## Funding

This study was supported by grants from the Research to Prevent Blindness and the United States National Eye Institute (R01 EY014999).

## Declarations

## Competing interests

The authors declare no competing interests.

**Table.**

## Additional information

**Supplementary Information** The online version contains supplementary material available at <https://doi.org/10.1038/s41598-024-75289-1>.

**Correspondence** and requests for materials should be addressed to G.Y.

**Reprints and permissions information** is available at [www.nature.com/reprints](http://www.nature.com/reprints).

**Publisher's note** Springer Nature remains neutral with regard to jurisdictional claims in published maps and institutional affiliations.

**Open Access** This article is licensed under a Creative Commons Attribution-NonCommercial-NoDerivatives 4.0 International License, which permits any non-commercial use, sharing, distribution and reproduction in any medium or format, as long as you give appropriate credit to the original author(s) and the source, provide a link to the Creative Commons licence, and indicate if you modified the licensed material. You do not have permission under this licence to share adapted material derived from this article or parts of it. The images or other third party material in this article are included in the article's Creative Commons licence, unless indicated otherwise in a credit line to the material. If material is not included in the article's Creative Commons licence and your intended use is not permitted by statutory regulation or exceeds the permitted use, you will need to obtain permission directly from the copyright holder. To view a copy of this licence, visit <http://creativecommons.org/licenses/by-nc-nd/4.0/>.

© The Author(s) 2024